RESEARCH PAPER

Acta Neurobiol Exp 2022, 82: 358–372
DOI: 10.55782/ane-2022-034

since 1928 ACTA NEUROBIOLOGIÆ EXPERIMENTALIS

HIF-1α protects PC12 cells from OGD/R-induced cell injury by regulating autophagy flux through the miR-20a-5p/KIF5A axis

Jing-Wei Cao[1], Zhan-Bin Tang[1], Ji-He Song[1], Jia-Lin Yao[2], Xiao-Meng Sheng[3], Zhi-Qiang Su[4]*

[1] Internal Medicine-Neurology, The First Affiliated Hospital of Harbin Medical University, Harbin, P.R. China,
[2] Department of Trauma Surgery, Harbin First Hospital, Harbin, P.R. China,
[3] Medicine-Neurology, Harbin Fourth Hospital, Harbin, P.R. China,
[4] Department of Neurology, The First Affiliated Hospital of Harbin Medical University, Harbin, P.R. China,
** Email: zhqian789@163.com*

Hypoxia inducible factor 1α (HIF-1α) has been reported to play a key role in protecting neurons from ischaemic injury. However, the exact molecular mechanisms remain largely unclear. PC12 cells were exposed to oxygen glucose deprivation/reoxygenation (OGD/R) conditions to mimic ischaemic injury *in vitro*. The expression of the HIF-1α mRNA, miR-20a-5p, and kinesin family member 5A (KIF5A) mRNA was tested using qRT–PCR. Levels of the HIF-1α, LC3I/II, P62, LAMP2, cathepsin B (CTSB) and KIF5A proteins were determined using western blotting. The CCK-8 assay was conducted to assess PC12 cell viability. DQ-Red-BSA and LysoSensor Green DND-189 dyes were employed to measure the proteolytic activity and pH of lysosomes, respectively. The interaction between miR-20a-5p and HIF-1α or KIF5A was verified by performing chromatin immunoprecipitation (ChIP) and/or dual-luciferase reporter assays. TUNEL staining was adopted to assess PC12 cell death. GFP-LC3 and RFP-GFP-LC3 probes were used to examine the autophagy status and autophagy flux of PC12 cells. A rat middle cerebral artery occlusion-reperfusion (MCAO/R) model was established to investigate the role of the HIF-1α/miR-20a-5p/KIF5A axis in ischaemic stroke *in vivo*. OGD/R exposure initiated PC12 cell autophagy and injury. HIF-1α expression was substantially increased in PC12 cells after OGD/R exposure. Overexpression of HIF-1α reversed the effects of OGD/R on reducing cell viability, blocking autophagy flux and inducing lysosome dysfunction. These rescue effects of HIF-1α depended on KIF5A. HIF-1α negatively regulated miR-20a-5p expression by targeting its promoter region, and miR-20a-5p directly targeted and negatively regulated the KIF5A mRNA. Overexpression of miR-20a-5p abolished the effects of HIF-1α on rescuing OGD/R-induced injury in PC12 cells. The effects of the HIF-1α/miR-20a-5p/KIF5A axis were verified in MCAO/R rats. HIF-1α protects PC12 cells from OGD/R-induced cell injury by regulating autophagy flux through the miR-20a-5p/KIF5A axis.

Key words: ischaemic stroke, HIF-1α, OGD/R, autophagy flux, KIF5A

INTRODUCTION

Stroke, an acute disorder caused by an impaired blood supply in the brain, has been reported to be the fifth leading cause of death and the main cause of acquired disability in adults worldwide (Guzik and Bushnell, 2017). The annual incidence of stroke is approximately 795,000 in the United States, with an average of one case diagnosed per minute, according to the estimate of the American Heart Association (Sun et al., 2018b). In China, its annual incidence is approximately 1115 per million, with a mortality rate of approximately 115 per million (Sun et al., 2018b). Ischaemic stroke accounts for approximately eighty percent of all stroke cases, and rapid thrombolysis is currently used as the most important therapeutic option for ischaemic stroke (Rodrigo et al., 2013). Nevertheless, restoration of the blood supply after ischaemia may result in serious secondary damage

Received 28 September 2020, accepted 22 March 2022

to the brain, mainly due to the impaired function of the blood–brain barrier (BBB) (Pan et al., 2007; Abu Fanne et al., 2010). Despite spending more than 70 billion dollars annually on the development of ischaemic stroke treatments, the results are still far from satisfactory (Sun et al., 2018b). Thus, developing novel therapeutic options for ischaemic stroke is still urgently needed.

Autophagy is a strictly regulated cellular process by which damaged intracellular organelles and aggregated proteins are transported to lysosomes by autophagosomes for degradation and recycling (Wang et al., 2018). By removing damaged cytosolic components, autophagy flux plays a critical role in maintaining cellular and metabolic homeostasis (Wang et al., 2018). Defects in the autophagy process are a common cause of cell death in the central nervous system (CNS), resulting in the occurrence of various CNS disorders, including ischaemic stroke (Li et al., 2018b; Wang et al., 2018). Evidence have revealed a key role for autophagy in regulating OGD/R-induced neuronal injury through various signalling cascades (Sun et al., 2018a; Wang et al., 2019). Moreover, autophagy activation induced by hyperbaric oxygen preconditioning substantially alleviates I/R injury in an animal study (Fang et al., 2019).

Hypoxia inducible factor 1α (HIF-1α) is an important transcription factor involved in regulating various biological events, such as angiogenesis, erythropoiesis and metabolism (Lee et al., 2004). It is rapidly degraded under normoxic conditions, while its degradation is repressed under hypoxic conditions, resulting in its accumulation in cells (Lee et al., 2004; Cunningham et al., 2012). HIF-1α has been identified as a critical protein protecting against cerebral ischaemia-induced injury based on accumulating *in vitro* evidence (Cunningham et al., 2012). However, researchers have not yet determined whether HIF-1α regulates autophagy flux during ischaemic stroke.

As a well-known gene regulator, microRNAs (miRNAs) have been reported to play a critical role in ischaemic stroke (Mirzaei et al., 2018). Evidence has revealed altered expression levels of numerous miRNAs in the blood and brain of both animals and humans after stroke (Li et al., 2018a). Moreover, the interaction between miRNAs and HIF-1α has been reported to alter the functional outcome of ischaemic stroke in animals (Zhang et al., 2020). As a common miRNA, miR-20a-5p mediates hypoxia-induced autophagy by regulating ATG16L1 in ischaemic kidney injury, while HIF-1α represses miR-20a-5p by targeting its promoter (Wang et al., 2015). Nevertheless, the role of miR-20a-5p in ischaemic stroke-induced cerebral injury remains unknown.

Kinesin family member 5A (KIF5A) was revealed to be a molecular motor associated with the intracellular movement of macromolecules and organelles (Yu et al., 2019). Recently, KIF5A overexpression was reported to alleviate trimethyltin chloride-induced neurotoxicity by restoring autophagy flux in Neuro-2a cells (Liu et al., 2020). Its role in regulating autophagy flux reminds us that KIF5A may play a role in ischaemic stroke. Moreover, according to the TargetScan (http://www.targetscan.org/vert_72/) prediction, KIF5A is targeted by miR-20a-5p. Thus, we speculated that HIF-1α, miR-20a-5p and KIF5A may function as an axis to regulate autophagy flux in ischaemic stroke.

In this study, HIF-1α was revealed to protect PC12 cells from oxygen glucose deprivation/reoxygenation (OGD/R)-induced injury by restoring autophagy flux. Mechanistically, HIF-1α targeted the promotor of miR-20a-5p and suppressed its expression. Moreover, miR-20a-5p targeted and regulated KIF5A mRNA expression in PC12 cells. In summary, HIF-1α protected PC12 cells from OGD/R-induced injury by regulating autophagy flux through the miR-20a-5p/KIF5A axis.

METHODS

Cell culture and oxygen glucose deprivation/reoxygenation (OGD/R) exposure

The PC12 cell line, which was purchased from the American Type Culture Collection, was cultured in Dulbecco's modified Eagle's medium (DMEM, Life Technologies, USA) supplemented with 1% penicillin/streptomycin and 10% foetal bovine serum (Gibco, USA), and maintained at 37°C in an incubator filled with 5% CO_2 and 95% O_2. For OGD/R treatment, PC12 cells were cultured with glucose- and serum-free culture medium in a hypoxic environment (95% N_2 and 5% CO_2) for 2 h, 4 h, or 6 h, and then cultured with normal culture medium in a normoxic environment (5% CO_2 and 95% O_2) for another 24 h. Cells cultured with normal culture medium in a normoxic environment were used as controls.

Quantitative real-time PCR (RT–PCR) analysis

Total RNA was isolated from PC12 cells lysed in TRIzol reagent (Thermo Fisher Scientific, USA) and then transcribed into cDNAs using a SuperScript VILO™ cDNA Synthesis Kit (Invitrogen, USA) after the examination of its quality. Relative expression of miR-20a-5p, the HIF-1α mRNA, and KIF5A mRNA was measured using the ABI7500 Fast Real-Time PCR System (PE Applied Biosystems) according to the instructions of TaqMan MicroRNA Assay Kit (for miRNAs, Thermo Fisher, USA) or SYBR Green PCR kit (for mRNAs, Takara, Japan). Gene expression was calculated using the

$2^{-\Delta\Delta Ct}$ method. GAPDH was used as an internal control for mRNAs, and U6 was used as an internal control for miRNAs. The sequences of the primers used in this study were as follows:
miR-20a-5p: Forward-5'-GGCGTAAAGTGCTTATAGTGC-3',
Reverse: 5'-GTGCAGGGTCCGAGGT-3';
HIF-1α: Forward-5'-GAAACTCCAAAGCCACTTCG-3',
Reverse-5'-CTGGGACTGTTAGGCTCAGG-3';
KIF5A: Forward-5'-AGATCCGCCGTCTCTACAAG-3',
Reverse: 5'-GCATCGTTCTCAGACTGCAG -3';
U6: Forward-5'-CTCGCTTCGGCAGCACA-3',
Reverse: 5'-AACGCTTCACGAATTTGCGT-3'; and
GAPDH: Forward-5'-GCAAGTTCAACGGCACAG-3',
Reverse: 5'-GCCAGTAGACTCCACGACAT-3'.

Cell transfection

A HIF-1α overexpression vector was established by inserting the full-length HIF-1α sequence into the pcDNA3.1 vector, and a short hairpin RNA (shRNA) was designed to target the sequence of the HIF-1α or KIF5A gene, which was referred to as sh-HIF-1α or sh-KIF5A, respectively. The HIF-1α overexpression vector, sh-HIF-1α, sh-KIF5A, miR-20a-5p mimics, and miR-20a-5p inhibitor, as well as their corresponding negative controls, were all supplied by Life Technologies (USA). For transfection, cells were transfected with the indicated oligonucleotides using Lipofectamine 3000 reagent (Thermo Fisher Scientific, USA) according to the manufacturer's procedures.

Western blot

Proteins were extracted from PC12 cells after lysis in RIPA buffer (Beyotime, China), and then the protein concentration was determined using the BCA Protein Assay Kit (Solarbio, China). Protein samples (50 μg) were subsequently separated on 10% SDS–PAGE gels followed by transfer to nitrocellulose membranes. After blocking with 5% low-fat milk for 2 h, the membranes were incubated with primary antibodies against LC3 (1:1000, #2775, Cell Signaling Technology, USA), P62 (1:1000, #16177, Cell Signaling Technology), LAM2 (1:2000, ab13524, Abcam, USA), cathepsin B (CTSB) (1:3000, ab125067, Abcam) and β-actin (1:5000, ab179467, Abcam) for 12 h at 4°C. Afterwards, membranes were incubated with HRP-conjugated secondary antibodies at room temperature for 2 h. Enhanced chemiluminescence reagent (EMD Millipore, USA) was employed to visualize bands, and ImageJ software (National Institutes of Health, USA) was used to analyse band intensities.

Cell counting kit-8 (CCK-8) assay

CCK-8 was adopted to determine the viability of treated PC12 cells. Briefly, PC12 cells were collected and seeded into 96-well plates (5000 cells/well) after the indicated treatment. After a 2 h incubation at 37°C, 10 μl of CCK-8 reagent were added to each well and incubated at 37°C for another 1 h. Absorbance was determined at 450 nm using a microplate reader (Bio-Rad, USA).

DQ-Red-BSA staining

DQ-Red-BSA dye (Invitrogen, D12051, USA) was employed to assess the proteolytic activity of lysosomes in treated PC12 cells according to the manufacturer's protocol. Briefly, treated PC12 cells were collected and incubated with DQ-Red-BSA dye for 2 h followed by visualization with a confocal microscope (Nikon, Japan). DQ-Red-BSA-positive spots were analysed using CellProfiler (Version 3.0, open source software).

Lysosomal pH measurement

LysoSensor Green DND-189 dye was employed to measure the lysosomal pH in PC12 cells. Briefly, treated PC12 cells were seeded into 24-well plates and incubated with 1 μM LysoSensor Green DND-189 dye (Invitrogen, USA) in culture medium for 30 min. Next, the cells were washed with PBS and analysed using a fluorescence microscope (Nikon, Japan).

Dual-luciferase reporter assay

The interaction between miR-20a-5p and KIF5A was verified using a dual-luciferase reporter assay in PC12 cells. Briefly, the wild-type (WT) and mutant (MUT) miR-20a-5p binding sites in KIF5A were subcloned into the pGL3 vector individually and referred to as WT-KIF5A and MUT-KIF5A. PC12 cells were co-transfected with miR-20a-5p mimics or NC mimics and WT-KIF5A or MUT-KIF5A using Lipofectamine 3000 reagent. Twenty-four hours after transfection, the luciferase activity of PC12 cells was measured using a Dual-Luciferase Reporter Assay System (Promega, Madison, WI). Recombinant reporter plasmids were established by inserting the WT or MUT miR-20a-5p sequence into the pGL3 vector and referred to as WT-miR-20a-5p and MUT-miR-20a-5p to verify the interaction between miR-20a-5p and HIF-1α. PC12 cells were co-transfected with WT-miR-20a-5p or MUT-miR-20a-5p and HIF-1α or sh-HIF-1α. Forty-eight hours after transfection, the lu-

ciferase activity of PC12 cells was measured using a Dual-Luciferase Reporter Assay System.

Chromatin immunoprecipitation (ChIP) assay

A ChIP assay kit (Beyotime, China) was employed to verify the interaction between HIF-1α and the miR-20a-5p promoter. Briefly, treated PC12 cells were cross-linked with 1% formaldehyde for 10 min and then quenched with glycine (125 mM, 5 min). Next, the cells were centrifuged at 1500 rpm for 10 min, followed by lysis in lysis buffer containing protease inhibitors (10 min) on ice. Cell lysates were then sonicated into chromatin fragments and centrifuged at 12000 rpm for 10 min. The supernatant was diluted with ChIP buffer containing PMSF (1 mM) and Protein A/G agarose/salmon sperm DNA. The mixture was centrifuged again at 1000 rpm for 2 min, and then the supernatant was immunoprecipitated with an anti-HIF-1α antibody overnight. The immunoprecipitated DNA was eluted, and PCR was performed using primers that spanned the sequence of HIF-1α binding sites in the promoter of miR-20a-5p. The sequences of the primers were as follows: miR-20a-5p: Forward: 5'-GGC GTA AAG TGC TTA TAG TGC-3' and Reverse: 5'-GTG CAG GGT CCG AGG T-3'.

Assessment of autophagy using GFP-LC3 and RFP-GFP-LC3 probes

PC12 cells at 80% confluence were transfected with the GFP-LC3 plasmid using Lipofectamine 3000 (Invitrogen, USA) to quantify autophagy. Forty-eight hours after transfection, PC12 cells were seeded on poly-L-LYS-coated coverslips and fixed with 4% PFA in PBS for 30 min. Next, GFP puncta formation in PC12 cells was detected under a confocal microscope (Olympus, Japan). The percentage of GFP puncta was calculated in 6 fields selected randomly, and significance was determined from three repeated independent experiments. For the RFP-GFP-LC3 analysis, PC12 cells were infected with lentiviruses expressing RFP-GFP-LC3 (GeneChem, Shanghai, China) for 36 h and screened with puromycin for 72 h. PC12 cells stably expressing GFP-RFP-LC3 were seeded on poly-L-LYS-coated coverslips and then fixed with 4% PFA in PBS for 30 min. Signals were also detected under a confocal microscope (Olympus, Japan).

TUNEL staining

An in-situ Cell Death Detection Kit (Roche Diagnostics Corporation, USA) was adopted to assess the death of PC12 cells according to the manufacturer's instructions. After TUNEL staining, PC12 cells were counterstained with DAPI (Sigma, USA), and the signals were examined using a confocal microscope (Olympus, Japan). TUNEL-positive cells were counted in 6 randomly selected fields, and the average number of dead cells was calculated.

Rat middle cerebral artery occlusion-reperfusion (MCAO/R) model

Sprague–Dawley rats (male, 250-300 g) were supplied by the First Affiliated Hospital of Harbin Medical University. Animals were housed in groups of 3 per cage at a constant temperature 22 ± 2°C with a 12 h light/dark cycle. The common carotid artery was isolated after anaesthesia with 10% chloral hydrate (i.p., 350 mg/kg), and the right external carotid artery branches were separated to establish the MCAO/R model. The internal carotid artery was ligated with a 4-0 nylon monofilament suture to occlude the middle cerebral artery. After 2 h of MCAO, the suture was removed for reperfusion for 24 h.

Assessment of neurological deficits

The neurological deficits of MCAO/R animals were assessed by calculating neurological severity scores, which ranged from 0 to 4: 0, no obvious symptoms; 1, front paw cannot be fully extended; 2, animal circles to one side while walking; 3, animal leans to one side while walking; and 4, animal cannot walk or loses consciousness.

Analysis of the infarct volume

After MCAO/R treatment, the brains were quickly removed from the animals and cut into 1 mm slices using a Leica Biosystems vibratome (VT1200s, Leica, Germany). Then, brain slices were incubated with 2,3,5-triphenyltetrazolium chloride (TTC) solution (2%) for 1 followed by another 1 h incubation with 4% paraformaldehyde. After washes with PBS, brain slices were photographed and analysed using ImageJ software (NIH, USA).

Statistical analysis

Data are presented as the means ± standard deviations (SD) and were analysed using GraphPad Prism software (Version 7.0, USA) with Student's *t* test or one-way analysis of variance (ANOVA) followed by Tukey's *post hoc* test. $P<0.05$ was considered statistically significant.

RESULTS

OGD/R induced PC12 cell injury by initiating autophagy

Western blot analysis was performed to measure the levels of autophagy-related proteins (LC3 and p62) and assess the effects of OGD/R exposure on PC12 cell autophagy. The results indicated that OGD/R exposure significantly increased the LC3-II/I ratio and p62 expression over time (Fig. 1A). The autophagy status of PC12 cells treated with OGD/R for 2, 4, and 6 h was further examined by performing a GFP-LC3 analysis. Compared to the control group, the GFP fluorescence intensities

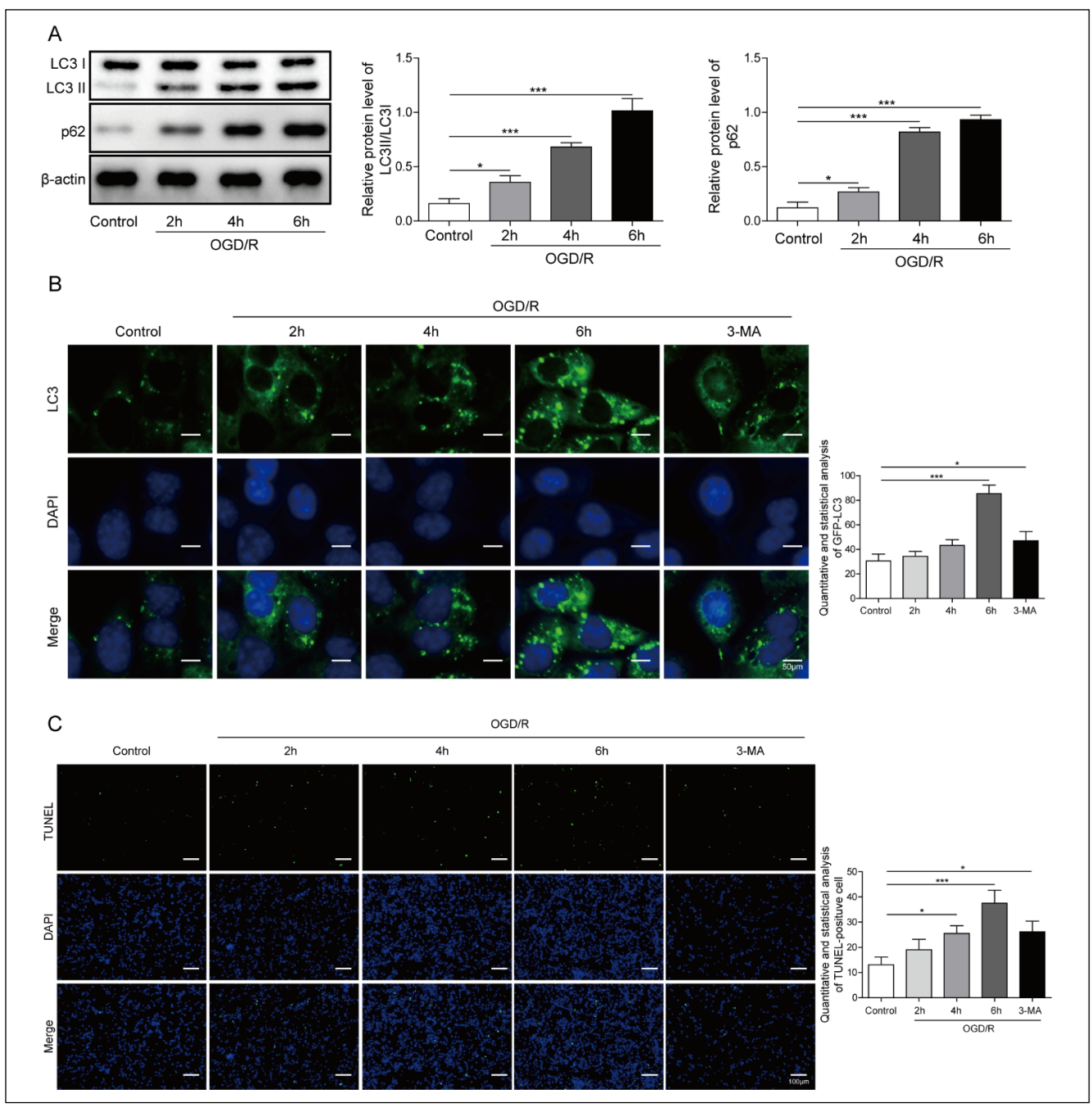

Fig. 1. OGD/R induced PC12 injury by initiating autophagy. (A) Western blot analysis of LC3 and P62 expression levels in PC12 cells after 2, 4, and 6 h of OGD/R exposure. (B) The autophagy status of PC12 cells treated with OGD/R for 2, 4, and 6 h was examined by analysing GFP-LC3 puncta. (C) TUNEL staining was applied to evaluate PC12 cell death under OGD/R conditions (6 h) in the presence or absence of 3-MA (pretreatment, 30 min, 10 mM). N=3; *p<0.05 or ***p<0.001.

were increased at 6 h after OGD/R exposure (Fig. 1B), indicating that OGD/R exposure induced the accumulation of autophagosomes in PC12 cells, thus promoting autophagy. Moreover, by analysing the fluorescence of PC12 cells pretreated with 3-MA after 6 h of OGD/R exposure, we found that pretreatment of PC12 cells with 3-MA reduced the accumulation of autophagosomes induced by OGD/R (Fig. 1B). Additionally, we assessed the effects of OGD/R exposure on the death of PC12 cells using TUNEL staining. After 4 and 6 h of OGD/R treatment, the number of TUNEL-positive PC12 cells was remarkably increased compared to the control group (Fig. 1C). We evaluated the death of PC12 cells pretreated with 3-MA (10 mM, 30 min) under OGD/R conditions by performing TUNEL staining to further determine the causal relationship between OGD/R-induced injury and autophagy initiation. The 3-MA pretreatment alleviated OGD/R-induced PC12 cell death (Fig. 1C). These findings suggested that OGD/R induced PC12 cell injury by initiating autophagy.

HIF-1α overexpression alleviated the attenuated cell viability, blocked autophagy flux and lysosome dysfunction induced by OGD/R

First, we examined HIF-1α expression in PC12 cells after OGD/R exposure using qRT–PCR and western blotting. Compared to the control group, HIF-1α expression was substantially increased in the OGD/R group at both the mRNA and protein levels (Fig. 2A, B). Then, we estimated the effects of HIF-1α overexpression on the viability, autophagy flux, and lysosomal function of PC12 cells. Western blot results suggested that HIF-1α transfection remarkably upregulated HIF-1α expression in PC12 cells (Fig. 2C). In the CCK-8 assay, HIF-1α overexpression protected PC12 cells from the OGD/R-induced decrease in viability (Fig. 2D). Western blot analysis indicated that HIF-1α overexpression further increased the upregulation of HIF-1α induced by OGD/R and abolished the increases in the LC3-II/I ratio and p62 expression, as well as the downregulation of CTSB protein levels induced by OGD/R exposure in PC12 cells, which are proteins involved in the formation of autophagosomes and lysosomes, respectively (Fig. 2E). OGD/R-induced downregulation of LAMP2 was not altered by HIF-1α overexpression. A DQ-Red-BSA assay was performed to investigate the effects of HIF-1α overexpression on the proteolytic activity of lysosomes. DQ-Red-BSA is a protein complex that carries multiple fluorophores that autoquench each other. Once endocytosed and trafficked to lysosomes, the fluorophores will be separated. Therefore, an increase in the fluorescence intensity indicates increased proteolytic activity. HIF-1α overexpression in PC12 cells significantly reversed the attenuated proteolytic activity of lysosomes induced by OGD/R exposure (Fig. 2F). Autophagy is reported to be affected by the pH of lysosomes; thus, we measured the lysosomal pH of PC12 cells transfected with HIF-1α after OGD/R treatment using LysoSensor Green DND-189 dye, for which the fluorescent activity increases in a more acidic environment. HIF-1α overexpression reversed the decrease in the LysoSensor Green DND-189 fluorescence intensity in PC12 cells exposed to OGD/R (Fig. 2G). We infected PC12 cells with lentiviruses carrying expression cassettes that encode RFP-GFP-LC3 to further confirm the effects of HIF-1α on autophagy flux in PC12 cells. Before lysosome fusion, LC3-positive autophagosomes are observed as yellow puncta, and after fusion, autolysosomes are observed as red puncta. As expected, the number of autolysosomes was substantially increased in OGD/R-treated PC12 cells compared to the control group (Fig. 2H). Compared to the OGD/R group, HIF-1α overexpression significantly increased the number of autolysosomes in PC12 cells, while bafilomycin A1 treatment (100 nM, 1 h) blocked this change induced by HIF-1α overexpression (Fig. 2H). Based on these findings, HIF-1α overexpression alleviated the reduced cell viability and blockade of autophagy flux, as well as lysosome dysfunction, induced by OGD/R in PC12 cells.

KIF5A knockdown reversed the protective effects of HIF-1α on autophagy flux and lysosomal function

The qRT–PCR and western blot results indicated that OGD/R exposure significantly downregulated KIF5A at both the mRNA and protein levels, while HIF-1α transfection reversed the downregulation of KIF5A induced by OGD/R in PC12 cells (Fig. 3A, B). Moreover, we found that co-transfection of HIF-1α and sh-KIF5A abolished the upregulation of the KIF5A protein induced by HIF-1α transfection in PC12 cells using western blotting (Fig. 3C). The effects of HIF-1α on alleviating the OGD/R-induced decrease in cell viability were abolished by co-transfection of HIF-1α and sh-KIF5A (Fig. 3D). We evaluated the role of KIF5A in the effects of HIF-1α on autophagy flux in PC12 cells under OGDR/R conditions by detecting the expression of autophagy-related proteins in HIF-1α-overexpressing and sh-KIF5A co-transfected PC12 cells using western blotting. As shown in Fig. 3E, HIF-1α overexpression reversed the increases in the LC3-II/I ratio and p62 expression and the downregulation of CTSB and KIF5A induced by OGD/R exposure in PC12 cells, while these effects of HIF-1α overexpression were abrogated by sh-KIF5A. The HIF-1α overexpression-induced increase in proteolytic activity following OGD/R exposure was blocked by sh-KIF5A (Fig. 3F). Using LysoSensor Green

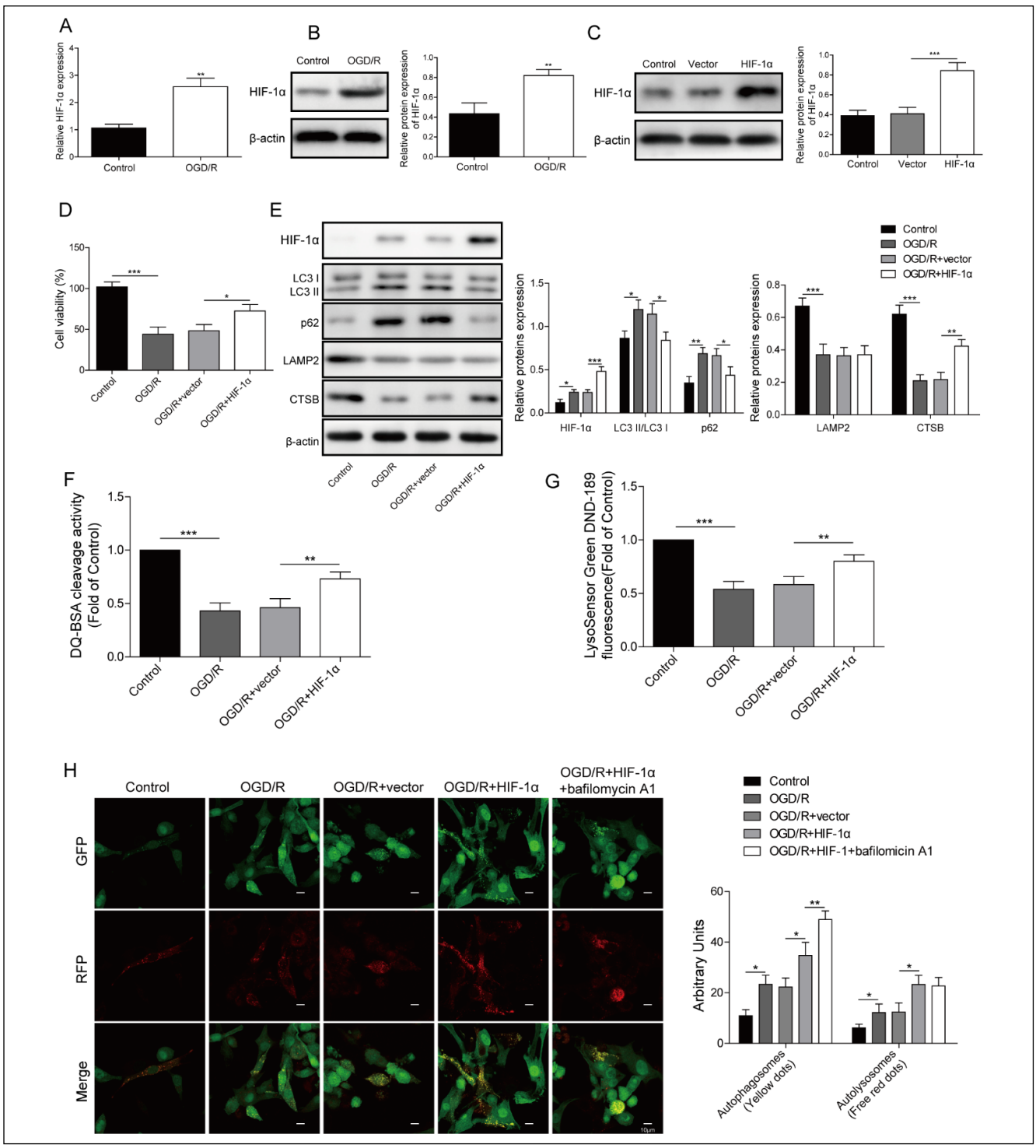

Fig. 2. HIF-1α overexpression alleviated the attenuated cell viability, blockade of autophagy flux and lysosome dysfunction induced by OGD/R. The relative expression of the HIF-1α (A) mRNA and (B) protein in OGD/R-treated PC12 cells was analysed using qRT–PCR and western blotting. (C) HIF-1α protein expression was measured in PC12 cells 48 h after transfection with HIF-1α overexpression vector. (D) The viability of HIF-1α-overexpressing PC12 cells was detected using a CCK-8 assay after OGD/R exposure. (E) Western blot analysis of HIF-1α, LC3, P62, LAMP2, and CTSB expression levels in HIF-1α-overexpressing PC12 cells after exposure to OGD/R. (F) Lysosomal activity of HIF-1α-overexpressing PC12 cells cultured under OGD/R conditions was evaluated using the fluorescent DQ™ Red-BSA dye. (G) LysoSensor Green DND-189 was employed to measure lysosome acidification in HIF-1α-overexpressing PC12 cells cultured under OGD/R conditions. (H) HIF-1α-overexpressing PC12 cells were transduced with the RFP-GFP-LC3 lentivirus and cultured under OGD/R conditions in the presence or absence of bafilomycin A1 (100 nM, 1 h) and then subjected to the evaluation of autophagy flux. N=3; *p<0.05, **p<0.01 or ***p<0.001.

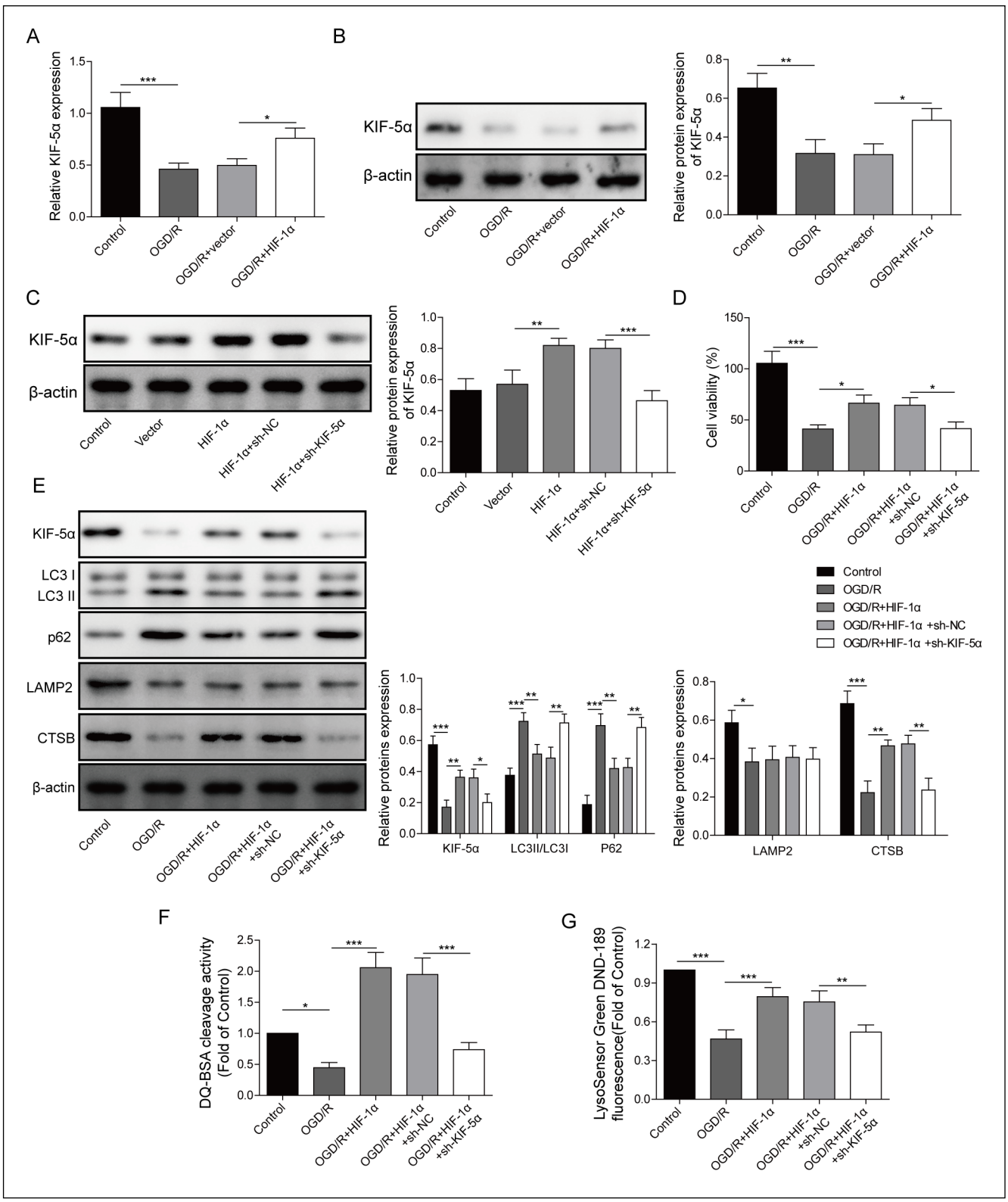

Fig. 3. KIF5A knockdown reversed the protective effects of HIF-1α on autophagy flux and lysosome function. The relative expression of the KIF5A (A) mRNA and (B) protein in PC12 cells transfected with the HIF-1α overexpression vector was detected after OGD/R exposure. (C) Relative expression of the KIF5A protein in HIF-1α-overexpressing and KIF5A knockdown PC12 cells. (D) PC12 cells transfected with pcDNA3.1-HIF-1α and sh-KIF5A were subjected to a viability assessment using CCK-8 after OGD/R exposure. (E) The expression of the KIF5A, LC3, P62, LAMP2, and CTSB proteins in PC12 cells. Lysosomal (F) proteolytic activity and (G) acidification in PC12 cells. N=3; *p<0.05, **p<0.01 or ***p<0.001.

DND-189 dye, we revealed that the effects of HIF-1α on alleviating OGD/R-induced increase in pH were abolished by sh-KIF5A (Fig. 3G). Therefore, the effects of HIF-1α overexpression on the decrease in cell viability, blockade of autophagy flux and lysosome dysfunction induced by OGD/R in PC12 cells depended on KIF5A.

KIF5A was targeted and negatively regulated by miR-20a-5p

The results of the qRT–PCR analysis showed a substantial increase in miR-20a-5p expression in PC12 cells exposed to OGD/R compared to that in PC12 cells cultured under normal conditions (Fig. 4A). Using the TargetScan database, we found that KIF5A may be a potential target of miR-20a-5p. Thus, we investigated whether KIF5A was regulated by miR-20a-5p using miR-20a-5p-overexpressing and miR-20a-5p-silenced PC12 cells. qRT–PCR analysis revealed that transfection of miR-20a-5p mimics or miR-20a-5p inhibitor caused significant upregulation and downregulation of miR-20a-5p, respectively, indicating good overexpression and knockdown efficiency (Fig. 4B). Using qRT–PCR and western blotting, we revealed that the overexpression of miR-20a-5p in PC12 cells resulted in a remarkable downregulation of the KIF5A mRNA and protein, while miR-20a-5p knockdown caused a significant upregulation of the KIF5A mRNA and

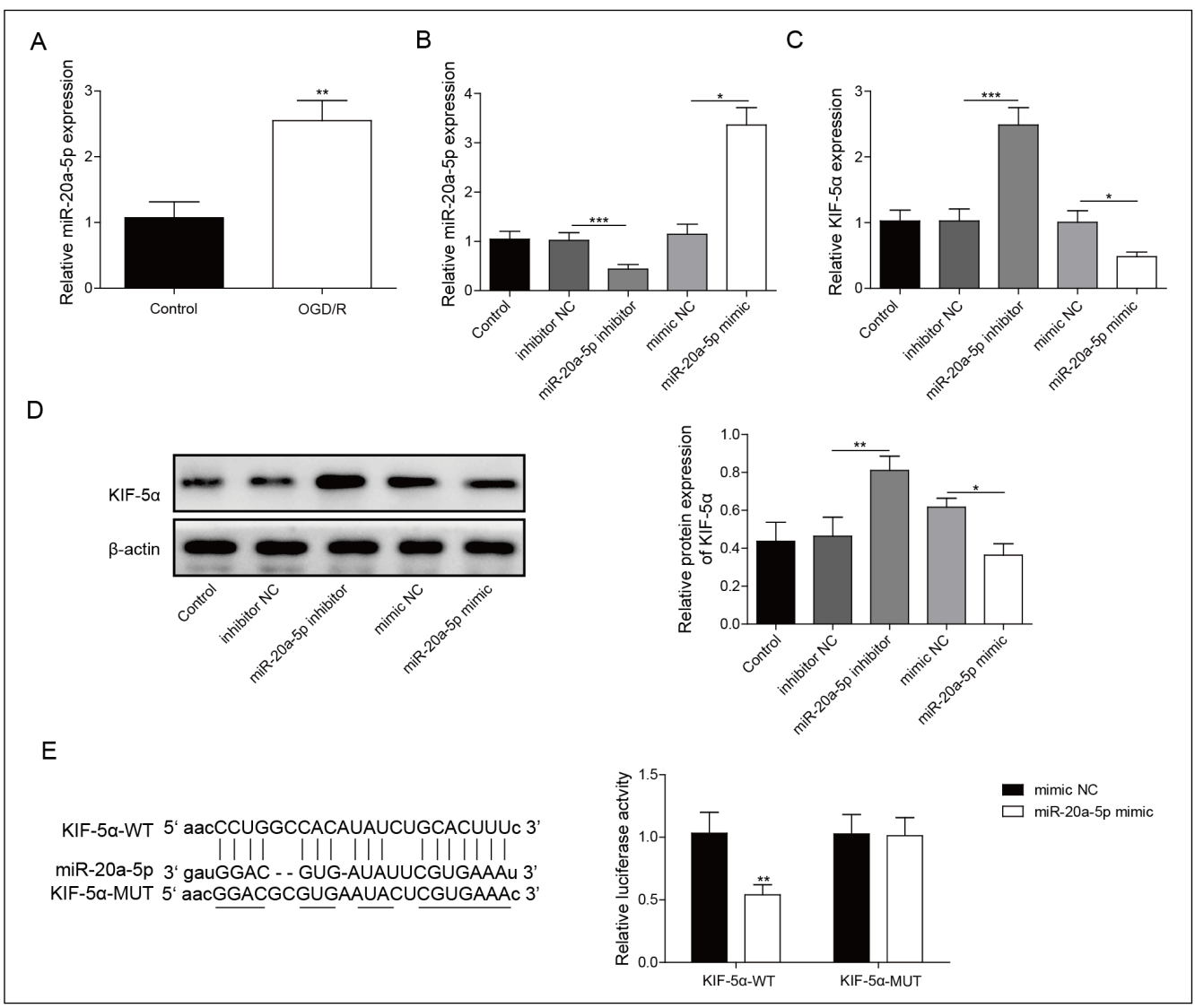

Fig. 4. KIF5A was targeted and negatively regulated by miR-20a-5p. (A) Relative expression of miR-20a-5p in PC12 cells cultured under normal or OGD/R conditions. (B) Relative miR-20a-5p expression in PC12 cells transfected with miR-20a-5p mimics or miR-20a-5p inhibitor. Relative expression of the KIF5A (C) mRNA and (D) protein in PC12 cells transfected with miR-20a-5p mimics or miR-20a-5p inhibitor. (E) Validation of the interaction between miR-20a-5p and KIF5A using a dual-luciferase reporter assay. N=3; *p<0.05, **p<0.01 or ***p<0.001.

protein (Fig. 4C, D), suggesting that KIF5A was negatively regulated by miR-20a-5p. A dual-luciferase reporter assay was performed in PC12 cells to further examine the interaction between KIF5A and miR-20a-5p. The luciferase activity of PC12 cells driven by KIF5A-WT was strongly decreased after the transfection of miR-20a-5p mimics but not mimic NC (Fig. 4E). These findings indicated that KIF5A was targeted and negatively regulated by miR-20a-5p.

HIF-1α negatively regulated miR-20a-5p expression by targeting its promoter

Next, the relationship between miR-20a-5p and HIF-1α in PC12 cells was investigated. The overexpression or knockdown efficiency of HIF-1α in PC12 cells was verified using qRT–PCR (Fig. 5A). We observed substantially decreased and increased miR-20a-5p expression in HIF-1α-overexpressing and HIF-1α-downregulated PC12 cells, respectively (Fig. 5B). The ChIP-qPCR assay revealed that HIF-1α could bind to the miR-20a-5p promoter region (Fig. 5C). Moreover, in the dual-luciferase reporter assay, HIF-1α overexpression or knockdown sharply reduced and enhanced the luciferase activity of PC12 cells driven by miR-20a-5p-WT, respectively (Fig. 5D). Based on these findings, HIF-1α negatively regulated miR-20a-5p expression by targeting its promoter.

miR-20a-5p overexpression reversed the protective effects of HIF-1α on autophagy flux and lysosomal function

As miR-20a-5p was targeted and repressed by HIF-1α in PC12 cells, we speculated that HIF-1α may

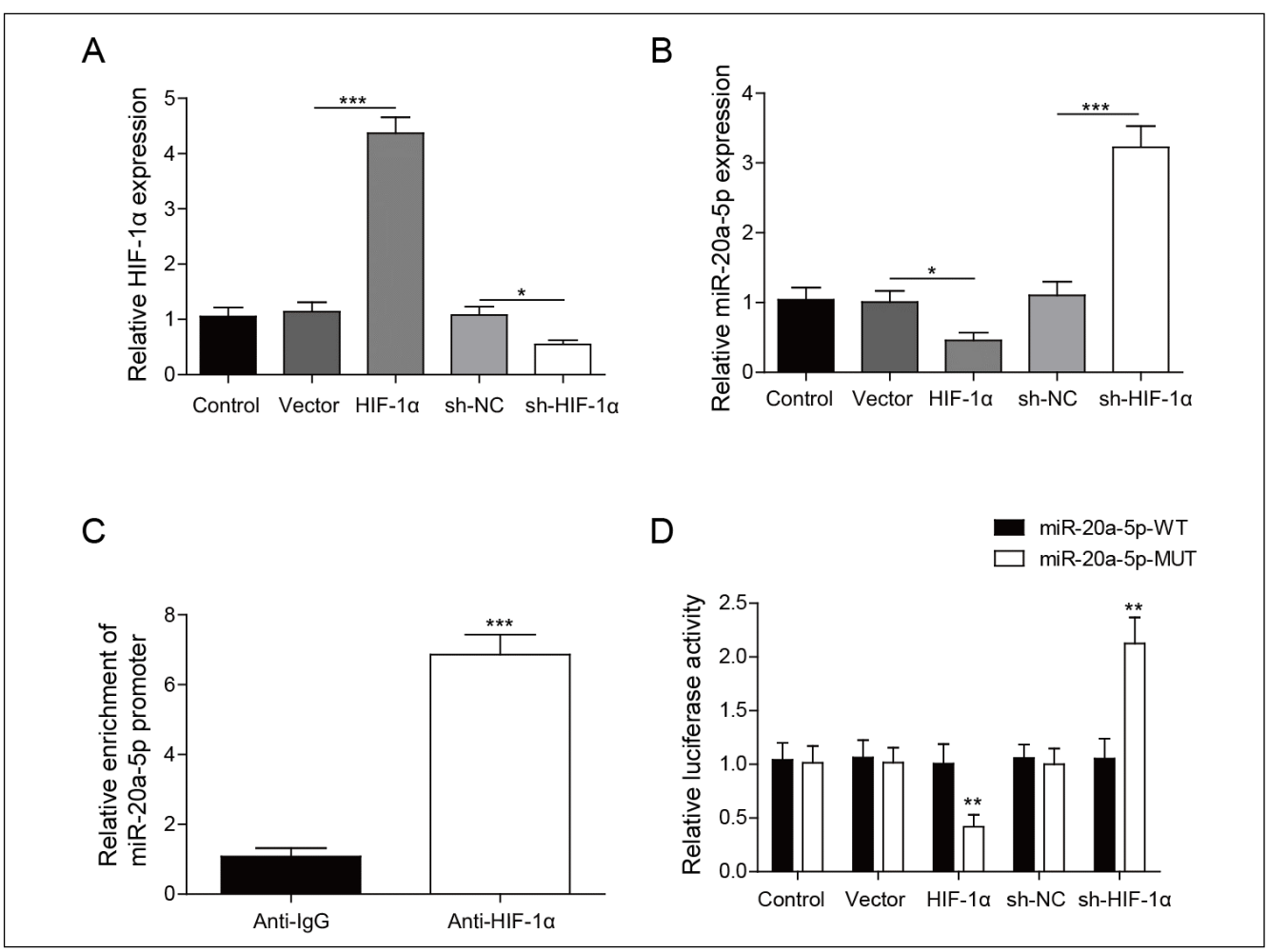

Fig. 5. HIF-1α negatively regulated miR-20a-5p expression by targeting its promoter. (A) Overexpression and knockdown efficiency of HIF-1α and sh-HIF-1α, respectively, were examined using qRT–PCR. (B) Relative level of miR-20a-5p in PC12 cells transfected with pcDNA3.1-HIF-1α and sh-HIF-1α. (C) ChIP and (D) dual-luciferase reporter assays were performed to examine the interaction between HIF-1α and the miR-20a-5p promoter. N=3; *p<0.05, **p<0.01 or ***p<0.001.

alleviate the OGD/R-induced decreases in cell viability and autophagy flux along with lysosome dysfunction by suppressing miR-20a-5p. We assessed the viability, autophagy flux and lysosomal function of PC12 cells co-transfected with a HIF-1α overexpression vector and miR-20a-5p mimics to verify this speculation. qRT–PCR

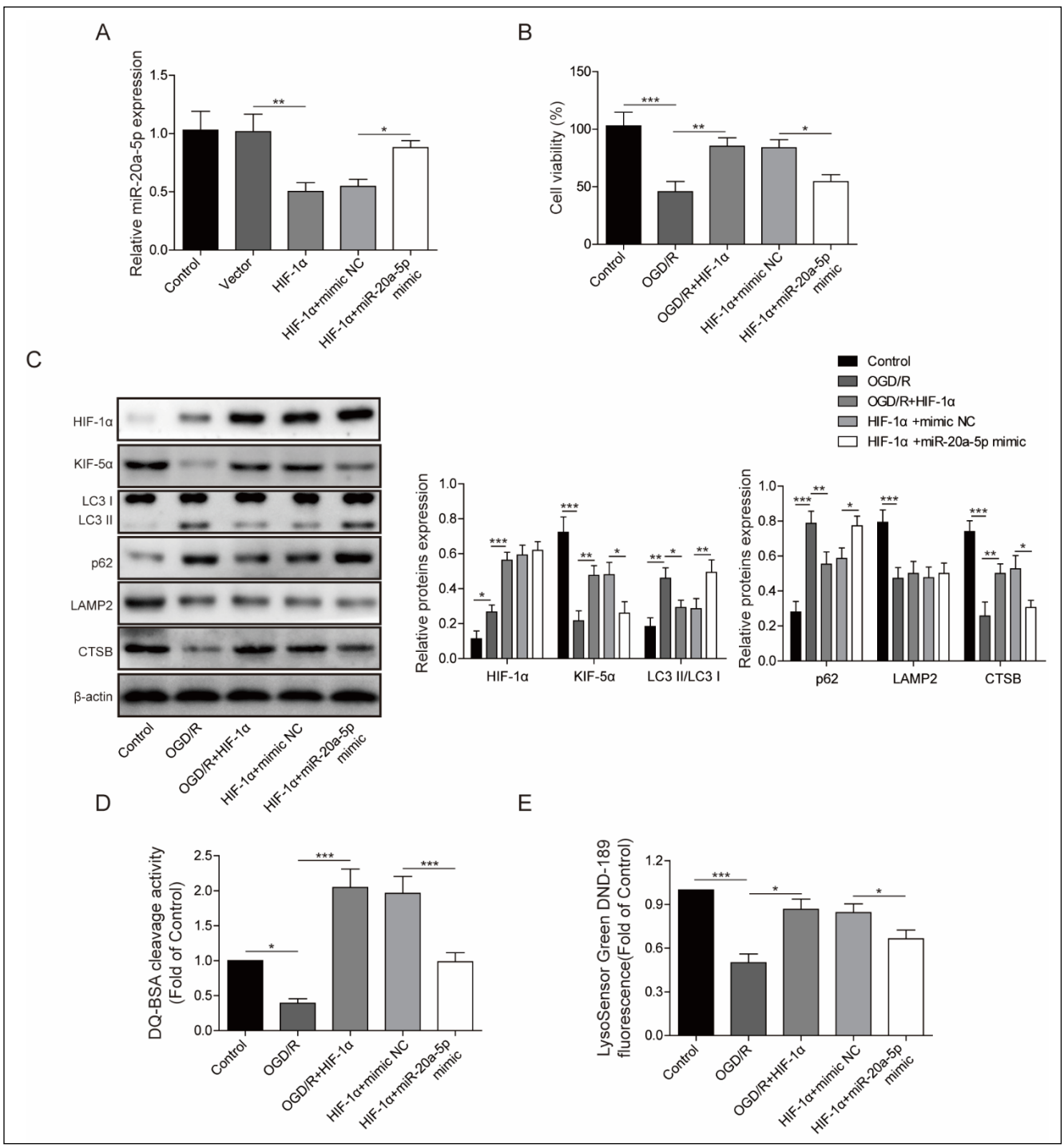

Fig. 6. miR-20a-5p overexpression reversed the protective effects of HIF-1α on autophagy flux and lysosome function. (A) Relative level of miR-20a-5p in PC12 cells transfected with pcDNA3.1-HIF-1α and miR-20a-5p mimics. (B) PC12 cells transfected with pcDNA3.1-HIF-1α and miR-20a-5p mimics were subjected to a cell viability assessment using CCK-8 after OGD/R exposure. (C) Levels of the HIF-1α, LC3, P62, LAMP2, and CTSB proteins in PC12 cells were detected using western blotting. The lysosomal (D) proteolytic activity and (E) acidification in PC12 cells transfected with pcDNA3.1-HIF-1α and miR-20a-5p mimics were examined after OGD/R exposure. N=3; *p<0.05, **p<0.01 or ***p<0.001.

analysis showed that co-transfection of HIF-1α and miR-20a-5p mimics reversed the downregulation of miR-20a-5p induced by HIF-1α overexpression (Fig. 6A). Moreover, co-transfection of HIF-1α and miR-20a-5p mimics dramatically counteracted the effects of HIF-1α overexpression on alleviating the reduced cell viability and autophagy flux along with lysosome dysfunction induced by OGD/R exposure (Fig. 6B-E). HIF-1α expression in PC12 cells cultured under OGD/R conditions was not affected by the transfection of miR-20a-5p (Fig. 6C). These results revealed that HIF-1α relieved PC12 cell injury, autophagy flux blockade and lysosome dysfunction by inhibiting miR-20a-5p expression following OGD/R exposure.

HIF-1α protected neurons from MCAO/R-induced neuronal injury by regulating autophagy flux through the miR-20a-5p/KIF5A axis *in vivo*

We evaluated the neurological deficits in MCAO/R rats injected with HIF-1α in the right lateral ventricle by analysing the neurological severity score to verify that HIF-1α protected against ischaemic stroke *in vivo*. The results indicated that the neurological deficits were significantly increased after the MCAO/R operation, while the HIF-1α treatment decreased the scores (Fig. 7A). Moreover, the brain infarct area of MCAO/R rats was examined using TTC staining. The MCAO/R operation caused massive infarction; however, in the MCAO/R rats injected with HIF-1α, the infarct volume was dramatically reduced (Fig. 7B). We also assessed neuronal death in brain tissues from MCAO/R rats by performing TUNEL staining. Compared to the sham group, neuronal death was significantly increased in the brain tissues of MCAO/R rats, while HIF-1α treatment alleviated neuronal injury in MCAO/R rats (Fig. 7C). We detected the expression of HIF-1α, miR-20a-5p, and KIF5A in brain tissues from MCAO/R rats treated with HIF-1α to verify the function of the HIF-1α/miR-20a-5p/KIF5A axis *in vivo*. The qRT–PCR results indicated that the MCAO/R operation increased the expression of HIF-1α and miR-20a-5p while decreasing the expression of KIF5A; moreover, HIF-1α treatment further increased the upregulation of HIF-1α while reversing the upregulation of miR-20a-5p and downregulation of KIF5A (Fig. 7D). Western blot analysis verified the alterations in levels of the HIF-1α and KIF5A proteins in the brain tissues of MCAO/R rats (Fig. 7E). Additionally, HIF-1α treatment abolished the increased LC3-II/I ratio and p62 expression, as well as the downregulation of CTSB protein levels induced by MCAO/R surgery (Fig. 7E). These findings confirmed the role of the HIF-1α/miR-20a-5p/KIF5A axis in ischaemic stroke *in vivo*.

DISCUSSION

Despite the numerous efforts over the past few decades in developing therapeutic options for ischaemic stroke, unfortunately, the available effective treatments to improve clinical outcomes of patients with ischaemic stroke are still currently extremely limited. Due to our poor understanding of the pathogenesis of ischaemic stroke in inducing cell injury, we are not currently able to improve the situation. Here, we showed that HIF-1α overexpression protected PC12 cells from OGD/R exposure-induced injury by restoring autophagy flux and lysosomal function through the miR-20a-5p/KIF5A axis, providing a novel potential therapeutic axis for ischaemic stroke treatment.

HIF-1α is stabilized in a hypoxic environment and transported into the nucleus to form a heterodimer with the β subunit of the aryl hydrocarbon receptor nuclear translocator, subsequently triggering the expression of more than sixty genes by binding hypoxia-response elements (Sharp et al., 2004). The neuroprotective effects of HIF-1α have been sufficiently documented by extensive studies both *in vitro* and *in vivo* (Shi, 2009; Lin et al., 2010). For instance, HIF-1α is upregulated in PC12 cells after OGD/R exposure, and overexpression of HIF-1α dramatically alleviated the OGD/R-induced injury of PC12 cells (Zhang et al., 2020). Moreover, repression of HIF-1α was reported to promote OGD/R-induced injury in PC12 cells (Cao et al., 2018). Additionally, *in vivo* delivery of an inhibitor (DMOG) of prolyl hydroxylases (PHDs), enzymes needed for HIF-1α degradation, increases the activation of HIF-1α, reduces the ischaemic infarct volume and reduces cell apoptosis after stroke in rats (Ogle et al., 2012). Here, we also provided evidence to support the neuroprotective effects of HIF-1α on OGD/R-induced injury in PC12 cells. Moreover, in this study, HIF-1α-mediated regulation of autophagy flux may play an important role in protecting PC12 cells from OGD/R-induced injury. Autophagy occurs not only in neurons but also in glial cells, and endothelial cells are closely associated with the pathology of ischaemic stroke; however, controversy exists regarding whether autophagy is beneficial or detrimental (Wang et al., 2018). In 2018, Lize Xiong et al. reported that activation of autophagy flux in astrocytes contributes to neuroprotective mechanisms after stroke (Liu et al., 2018). Moreover, activation of autophagy flux by HSPB8 alleviates ischaemia/reperfusion-induced injury by preventing the disruption of the BBB in a rat middle cerebral artery occlusion/reperfusion model (Li et al., 2019). Nevertheless, researchers have not determined whether the neuroprotective effects of HIF-1α on ischaemic stroke are mediated by autophagy activation. Here, we found that HIF-1α overexpression

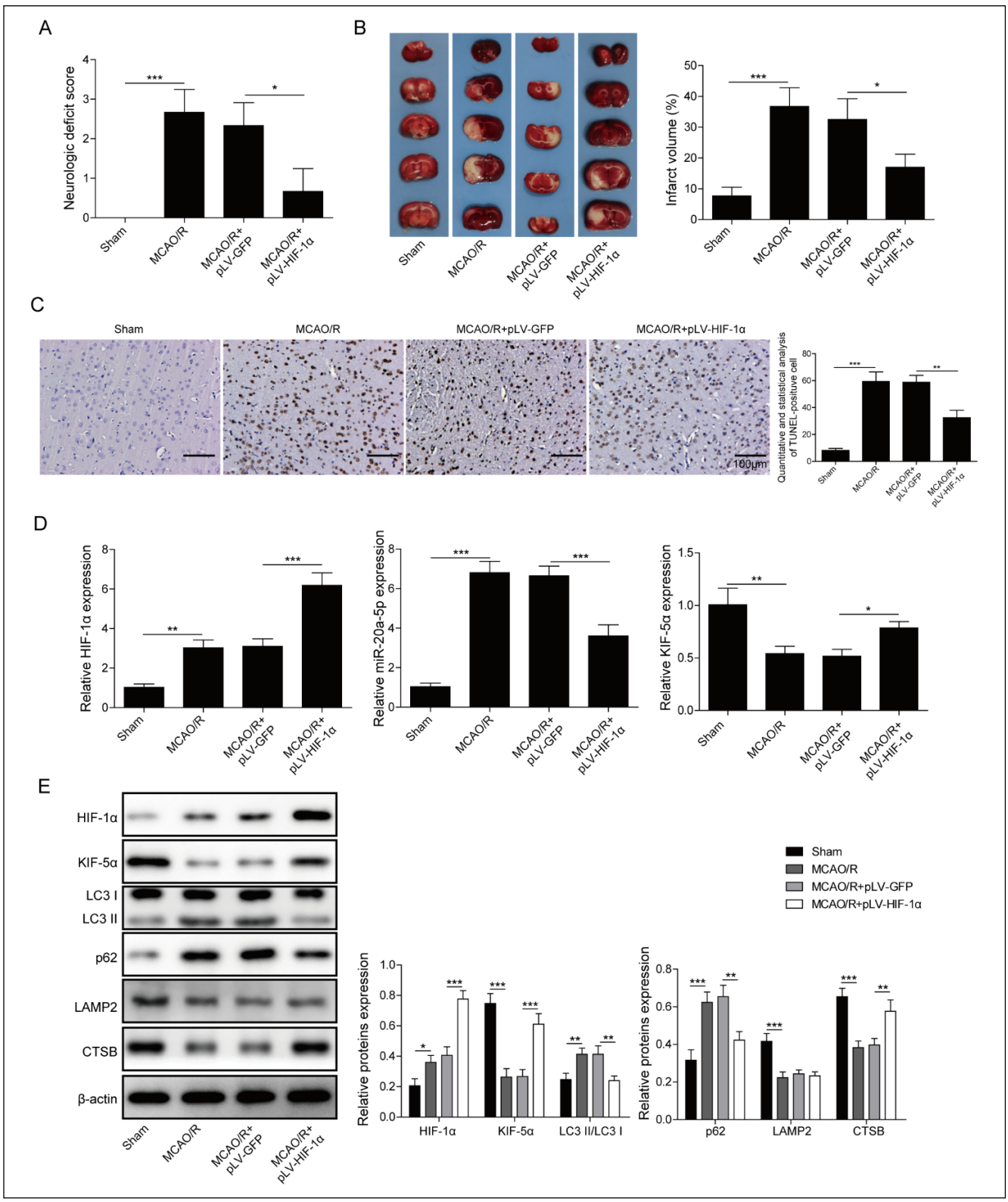

Fig. 7. HIF-1α protected neurons from MCAO/R-induced injury by regulating autophagy flux through the miR-20a-5p/KIF5A axis *in vivo*. (A) Quantitative analysis of neurological deficit scores in MCAO/R rats. (B) Representative images of TTC staining and quantitative analysis of the infarct volume in MCAO/R rats. (C) TUNEL staining was performed to evaluate the neuronal death in brain tissues from MCAO/R rats. (D) qRT–PCR analysis of HIF-1α, miR-20a-5p, and KIF5A expression in the brain tissues of MCAO/R rats. (E) Western blot analysis of HIF-1α, KIF5A, LC3, P62, LAMP2, and CTSB protein levels in the brain tissues of MCAO/R rats. **p*<0.05, ***p*<0.01 or ****p*<0.001.

reversed the OGD/R-induced autophagy flux blockade and lysosome dysfunction, implying that HIF-1α may protect PC12 cells from OGD/R-induced injury by activating autophagy flux.

According to previous studies, the underlying mechanisms of HIF-1α against ischaemic stroke may be based on its ability to promote the expression of several critical genes, such as glucose transporter, erythropoietin, and vascular endothelial growth factor (Jones et al., 2001; Bernaudin et al., 2002). Meanwhile, accumulating evidence suggests that miRNA-mediated gene expression may also play a role in stroke-induced injury (Rink and Khanna, 2011). For instance, miR-124 repression alleviates I/R-induced brain injury by modulating Ku70 expression (Zhu et al., 2014). Inhibition of miR-181b decreases ischaemic neuronal death by regulating HSPA5 and UCHL1 (Peng et al., 2013). In 2015, miR-20a-5p was reported to mediate hypoxia-induced autophagy in ischaemic kidney injury by regulating ATG16L. Moreover, this study revealed an inhibitory interaction of HIF-1α with miR-20a-5p (Wang et al., 2015). Consistently, in our study, we confirmed the binding of HIF-1α to the miR-20a-5p promoter and the inhibitory effect of HIF-1α on miR-20a-5p expression in PC12 cells. Additionally, we are the first to show that miR-20a-5p targeted and negatively regulated KIF5A expression.

KIF5A has been identified to be associated with the initiation and development of various diseases, such as cancer, epilepsy, and lateral sclerosis (Nakajima et al., 2012; Simone et al., 2018; Tian et al., 2019). Recently, KIF5A-dependent axonal transport was found to be a target in the trimethyltin chloride-induced blockade of autophagy flux and neurotoxicity (Liu et al., 2020). However, researchers have not determined whether KIF5A plays a role in I/R-induced injury. In our study, KIF5A knockdown reversed the protective effects of HIF-1α on autophagy flux and lysosome function under OGD/R conditions.

CONCLUSIONS

In summary, HIF-1α protected PC12 cells from OGD/R-induced injury by regulating autophagy flux through the miR-20a-5p/KIF5A axis, which represents a potentially novel axis to target for ischaemic stroke treatment.

ACKNOWLEDGEMENTS

This work was supported by Mechanism of long non coding RNA NEAT1 regulating microglia activation in cerebral ischemia-reperfusion injury (81771289). We would like to give our sincere gratitude to the reviewers for their constructive comments.

REFERENCES

Abu Fanne R, T Nassar, S Yarovoi, A Rayan, I Lamensdorf, M Karakoveski, P Vadim, M Jammal, D B Cines, AA Higazi (2010) Blood-brain barrier permeability and tPA-mediated neurotoxicity. Neuropharmacology 58: 972–980.

Bernaudin M, Y Tang, M Reilly, E Petit, FR Sharp (2002) Brain genomic response following hypoxia and re-oxygenation in the neonatal rat. Identification of genes that might contribute to hypoxia-induced ischemic tolerance. J Biol Chem 277: 39728–39738.

Cao YX, ZQ Wang, JX Kang, K Liu, CF Zhao, YX Guo, BH Jiao (2018) miR-424 protects PC-12 cells from OGD-induced injury by negatively regulating MKP-1. Eur Rev Med Pharmacol Sci 22: 1426–1436.

Cunningham LA, K Candelario, L Li (2012) Roles for HIF-1alpha in neural stem cell function and the regenerative response to stroke. Behav Brain Res 227: 410–417.

Fang Z, Y Feng, Y Li, J Deng, H Nie, Q Yang, S Wang, H Dong, L Xiong (2019) Neuroprotective autophagic flux induced by hyperbaric oxygen preconditioning is mediated by cystatin C. Neurosci Bull 35: 336–346.

Guzik A, C Bushnell (2017) Stroke epidemiology and risk factor management. Continuum 23: 15–39.

Jones NM, M Bergeron (2001) Hypoxic preconditioning induces changes in HIF-1 target genes in neonatal rat brain. J Cereb Blood Flow Metab 21: 1105–1114.

Lee JW, SH Bae, JW Jeong, SH Kim, KW Kim (2004) Hypoxia-inducible factor (HIF-1)alpha: its protein stability and biological functions. Exp Mol Med 36: 1–12.

Li F, B Yang, T Li, X Gong, F Zhou, Z Hu (2019) HSPB8 over-expression prevents disruption of blood-brain barrier by promoting autophagic flux after cerebral ischemia/reperfusion injury. J Neurochem 148: 97–113.

Li G, KC Morris-Blanco, MS Lopez, T Yang, H Zhao, R Vemuganti, Y Luo (2018a) Impact of microRNAs on ischemic stroke: From pre- to post-disease. Prog Neurobiol 163–164: 59–78.

Li H, J Wu, H Shen, X Yao, C Liu, S Pianta, J Han, C V Borlongan, G Chen (2018b) Autophagy in hemorrhagic stroke: Mechanisms and clinical implications. Prog Neurobiol 163–164: 79–97.

Lin CM, JH Chiu, IH Wu, BW Wang, CM Pan, YH Chen (2010) Ferulic acid augments angiogenesis via VEGF, PDGF and HIF-1 alpha. J Nutr Biochem 21: 627–633.

Liu M, H Pi, Y Xi, L Wang, L Tian, M Chen, J Xie, P Deng, T Zhang, C Zhou, Y Liang, L Zhang, M He, Y Lu, C Chen, Z Yu, Z Zhou (2020) KIF5A-dependent axonal transport deficiency disrupts autophagic flux in trimethyltin chloride-induced neurotoxicity. Autophagy: 1–22.

Liu X, F Tian, S Wang, F Wang, L Xiong (2018) Astrocyte autophagy flux protects neurons against oxygen-glucose deprivation and ischemic/reperfusion injury. Rejuvenation Res 21: 405–415.

Mirzaei H, F Momeni, L Saadatpour, A Sahebkar, M Goodarzi, A Masoudifar, S Kouhpayeh, H Salehi, HR Mirzaei, MR Jaafari (2018) MicroRNA: Relevance to stroke diagnosis, prognosis, and therapy. J Cell Physiol 233: 856–865.

Nakajima K, X Yin, Y Takei, DH Seog, N Homma, N Hirokawa (2012) Molecular motor KIF5A is essential for GABA(A) receptor transport, and KIF5A deletion causes epilepsy. Neuron 76: 945–961.

Ogle ME, X Gu, AR Espinera, L Wei (2012) Inhibition of prolyl hydroxylases by dimethyloxaloylglycine after stroke reduces ischemic brain injury and requires hypoxia inducible factor-1alpha. Neurobiol Dis 45: 733–742.

Pan J, AA Konstas, B Bateman, G A Ortolano, J Pile-Spellman (2007) Reperfusion injury following cerebral ischemia: pathophysiology, MR imaging, and potential therapies. Neuroradiology 49: 93–102.

Peng Z, J Li, Y Li, X Yang, S Feng, S Han, J Li (2013) Downregulation of miR-181b in mouse brain following ischemic stroke induces neuroprotection against ischemic injury through targeting heat shock protein A5 and ubiquitin carboxyl-terminal hydrolase isozyme L1. J Neurosci Res 91: 1349–1362.

Rink C, S Khanna (2011) MicroRNA in ischemic stroke etiology and pathology. Physiol Genomics 43: 521–528.

Rodrigo R, R Fernandez-Gajardo, R Gutierrez, J M Matamala, R Carrasco, A Miranda-Merchak, W Feuerhake (2013) Oxidative stress and pathophysiology of ischemic stroke: novel therapeutic opportunities. CNS Neurol Disord Drug Targets 12: 698–714.

Sharp FR, M Bernaudin (2004) HIF1 and oxygen sensing in the brain. Nat Rev Neurosci 5: 437–448.

Shi H (2009) Hypoxia inducible factor 1 as a therapeutic target in ischemic stroke. Curr Med Chem 16: 4593–4600.

Simone M, A Trabacca, E Panzeri, L Losito, A Citterio, MT Bassi (2018) KIF5A and ALS2 variants in a family with hereditary spastic paraplegia and amyotrophic lateral sclerosis. Front Neurol 9: 1078.

Sun B, H Ou, F Ren, Y Huan, T Zhong, M Gao, H Cai (2018a) Propofol inhibited autophagy through Ca(2+)/CaMKKbeta/AMPK/mTOR pathway in OGD/R-induced neuron injury. Mol Med 24: 58.

Sun Y, T Zhang, Y Zhang, J Li, L Jin, Y Sun, N Shi, K Liu, X Sun (2018b) Ischemic postconditioning alleviates cerebral ischemia-reperfusion injury through activating autophagy during early reperfusion in rats. Neurochem Res 43: 1826–1840.

Tian DW, ZL Wu, LM Jiang, J Gao, CL Wu, HL Hu (2019) KIF5A promotes bladder cancer proliferation in vitro and in vivo. Dis Markers 2019: 4824902.

Wang G, T Wang, Y Zhang, F Li, B Yu, J Kou (2019) Schizandrin protects against OGD/R-induced neuronal injury by suppressing autophagy: involvement of the AMPK/mTOR pathway. Molecules 24: 3624.

Wang IK, KT Sun, TH Tsai, CW Chen, SS Chang, TM Yu, TH Yen, FY Lin, CC Huang, CY Li (2015) MiR-20a-5p mediates hypoxia-induced autophagy by targeting ATG16L1 in ischemic kidney injury. Life Sci 136: 133–141.

Wang P, BZ Shao, Z Deng, S Chen, Z Yue, CY Miao (2018) Autophagy in ischemic stroke. Prog Neurobiol 163–164: 98–117.

Yu X, X He, LM Heindl, X Song, J Fan, R Jia (2019) KIF15 plays a role in promoting the tumorigenicity of melanoma. Exp Eye Res 185: 107598.

Zhang H, X Liu, F Yang, D Cheng, W Liu (2020) Overexpression of HIF-1alpha protects PC12 cells against OGD/R-evoked injury by reducing miR-134 expression. Cell Cycle 19: 990–999.

Zhu F, JL Liu, JP Li, F Xiao, ZX Zhang, L Zhang (2014) MicroRNA-124 (miR-124) regulates Ku70 expression and is correlated with neuronal death induced by ischemia/reperfusion. J Mol Neurosci 52: 148–155.